arXiv:1108.0919v2 [astro-ph.IM] 28 Dec 2012



Infrared Spectrograph
Technical Report Series

IRS-TR 11002: Calibration of the Acquisition Images from the Red Peak-Up Sub-Array

G.C. Sloan (1) & D.A. Ludovici (2) *

3 August, 2011†

Abstract

We present a calibration of the acquisition data obtained by the Red Peak-Up (PU) sub-array on the Infrared Spectrograph on *Spitzer*, based on repeated observations of three K giants. This calibration is tied directly to the most current infrared calibration based on data from the Multiband Imaging Photometer for *Spitzer*. An analysis of the responsivity of the Red PU sub-array reveals no detectable deviations from linearity in the most recent pipeline version, but older pipeline versions show evidence suggesting possible small non-linearities.

1 Introduction

One key step to the calibration of the Infrared Spectrograph (IRS; Houck et al. 2004) aboard the *Spitzer Space Telescope* (Werner et al. 2004) is the calibration of the acquisition images from the Red Peak-Up (PU) sub-array on

*(1) Infrared Spectrograph Science Center, Cornell University, (2) Department of Physics, West Virginia University; NSF REU Research Assistant, Astronomy Department, Cornell University

†With minor editorial corrections 23 Dec. 2011 and corrections 24 Dec. 2012 to the F_{24} value for HD 173511 in Table 3 and the references.

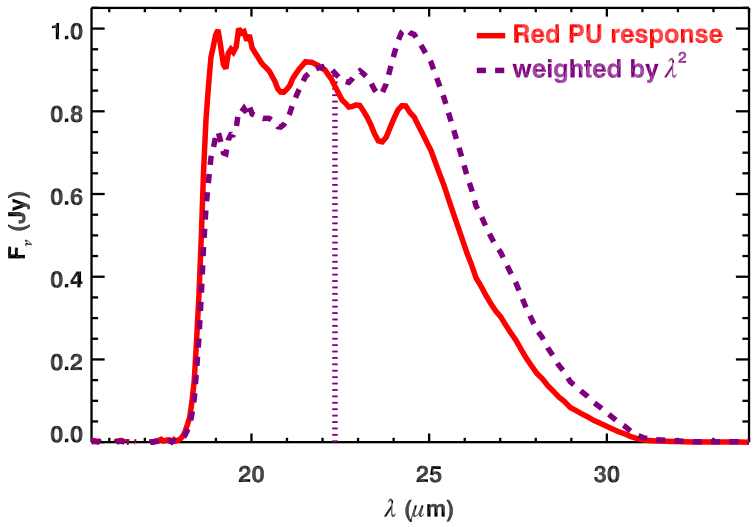


Figure 1 —The normalized responsivity of the Red PU sub-array for a bias voltage of 2.0 volts, as operated during the *Spitzer* mission. The solid curve shows the actual responsivity, while the dashed curve shows the responsivity $\times$ λ^2. The centroid of this latter curve is 22.35 μm (vertical dotted line), which we adopt as the effective wavelength of the Red PU filter.

the Short-Low module (SL). Our primary standards, HR 6348, HD 166780, and HD 173511 were observed repeatedly during the cryogenic *Spitzer* mission, and most of those observations began with target acquisition in the Red PU array. We can use these data to lock the overall photometry from these standards, and use that to photometrically calibrate their spectra.

2 Photometric calibration

To determine the effective wavelength of the Red PU filter, we multiply its responsivity (at a bias voltage of 2.0 volts) by λ^2, which approximates the long-wavelength behavior of a star. The centroid of the product is 22.35 μm, which we will adopt for the effective wavelength of the Red PU sub-array. Figure 1 illustrates the process.

We calibrate the Red PU data by tying our photometry to the calibration of the 24-μm filter on the Multiband Imaging Photometer for *Spitzer* (MIPS; Engelbracht et al. 2007, Rieke et al. 2008). MIPS-24 observed all three of our primary standards. Our procedure is to preserve the mean of the MIPS-

24 measurements, but to adjust the relative levels of the individual stars to reflect their brightnesses as observed in the Red PU images.

Our photometry follows the same procedure as described in IRS-TR 11001 (Sloan & Ludovici 2011). PU data were obtained in two sets of three images. For each set, we produced a median image, then performed aperture photometry using a four-pixel source radius and a seven-pixel radius for the sky annulus. In cases where the photometry from the initial (acquisition) image differed from the second (sweet-spot) image by more than 1.5%, we rejected the initial image from further consideration. Data obtained after IRS Campaign 14 have been corrected for the small variations in responsivity described in IRS-TR 1101, using divisive corrections of 0.9826 (Camp. 15–34) and 0.9929 (Camp. 35–61).

Table 1—Relative brightnesses of standards

Standard	**Spec.**		**Photometric signal (DN/s)**	
star	**class**	**Measurements**	**IRS Red PU**	**MIPS-24**
HR 6348	K1 III	163	1934.2 ± 2.1	30230 ± 122
HD 166780	K4 III	79	1950.4 ± 4.5	30650 ± 884
HD 173511	K5 III	217	2033.2 ± 2.0	31650 ± 124

Standard	**Normalized signal**	
star	**IRS Red PU**	**MIPS-24**
HR 6348	0.9802 ± 0.0011	0.9801 ± 0.0040
HD 166780	0.9870 ± 0.0023	0.9937 ± 0.0287
HD 173511	1.0328 ± 0.0010	1.0262 ± 0.0040

Table 1 presents the resulting photometry, both in digital units from the images and normalized to unity. Table 1 also presents similar results from the MIPS-24 data published by Engelbracht et al. (2007), using their calibration of 6.92×10^{-6} Jy (s/DN). The uncertainties in Table 1 are the uncertainties in the mean, and for the PU data, the lower values reflect the large number of (unrejected) observations.

Table 2—Ideal flux densities

Standard star	**Normalized flux density**	**Measured F_{24} (mJy)**	**Ideal F_{24} (mJy)**	**Ideal F_{22} (mJy)**
HR 6348	0.9813 ± 0.0029	209.2 ± 0.8	209.4 ± 0.6	235.0 ± 0.6
HD 166780	0.9881 ± 0.0023	212.1 ± 6.1	210.9 ± 0.5	236.7 ± 0.5
HD 173511	1.0306 ± 0.0029	219.0 ± 0.9	220.0 ± 0.6	246.9 ± 0.6

To combine the normalized signal in the 22–24 μm region for the three sources, we took a simple average of the IRS PU and MIPS-24 photometry for HR 6348 and HD 173511. For HD 166780, we adopted the value from the IRS PU images alone, due to the much higher uncertainty in the MIPS data. Table 2 presents the adopted normalized flux densities for the three standards, shifted up 0.0011 to preserve a mean of 1.0. The mean of the measured MIPS-24 data is 213.4 mJy, and the product of this mean and our normalized flux densities is the ideal flux density of the standards in the MIPS-24 filter. To determine the ideal flux density in the IRS Red PU filter, we scale the ideal MIPS-24 values by $1/\lambda^2$, assuming effective wavelengths of 22.35 and 23.675 μm.

The mean ratio of the ideal 22-um flux densities to the photometry with a four-pixel aperture gives a calibration of $1.2151 \pm 0.0008 \times 10^{-4}$ Jy (s/DN) for the IRS Red PU array.

3 Linearity

The samples of IRS standard stars observed with the Red PU array and the stars with MIPS-24 photometry observed by Engelbracht et al. (2007) have ten objects in common. Table 3 lists their photometry with both instruments. The photometry for the three K giants used in the calibration above differs slightly because none of the data have been rejected. The fluxes span a factor of nearly eight, which allows us to investigate the linearity of the reponsivity of the Red PU sub-array over nearly an order of magnitude. The last column of Table 3 gives the ratio of the Red PU photometry to the MIPS-24 photometry, after scaling the MIPS data by $1/\lambda^2$.

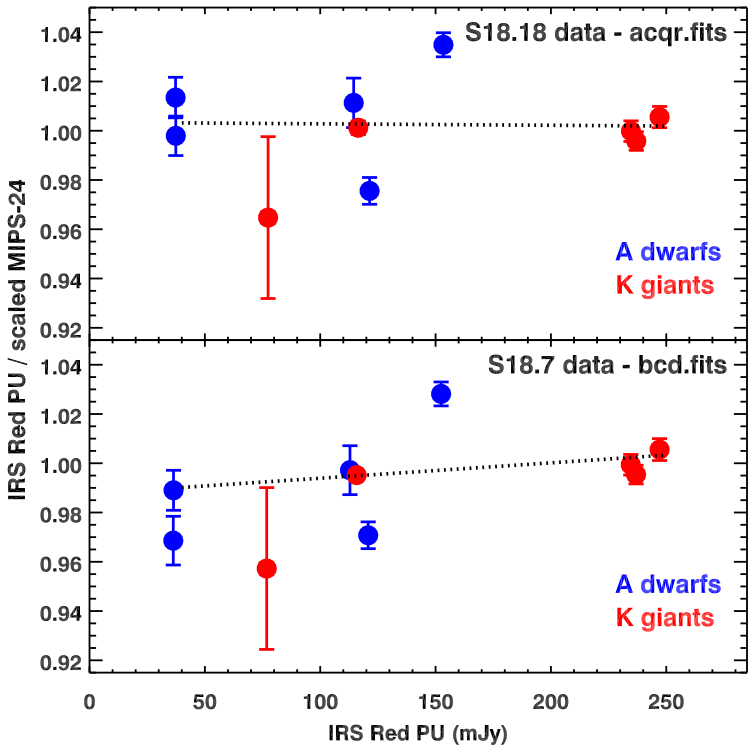


Figure 2 —The ratio of the IRS Red PU photometry to the MIPS-24 photometry (after scaling the MIPS data to account for the difference in wavelength), plotted vs. the PU flux density. The top panel plots the data given in Table 3, which are the S18.18 PU data, processed from the "acqr.fits" files. The bottom panel shows the S18.7 PU data, processed from the "bcd.fits" files. The dotted lines are lines fitted to the data, accounting for the uncertainties. No evidence for non-linearities in the response function are evident in the top panel, but the bottom panel does suggest a possible problem with the use of older pipeline versions of the PU data.

Table 3—Red PU and MIPS-24 photometry

Standard star	**IRS Red PU F_ν (mJy)**	**MIPS-24 F_ν (mJy)**	**IRS Red PU / scaled MIPS-24**
21 Lyn	114.5 ± 0.5	100.9 ± 0.9	1.011 ± 0.010
26 UMa	153.4 ± 0.2	132.1 ± 0.6	1.035 ± 0.005
HR 4138	121.4 ± 0.4	110.9 ± 0.5	0.976 ± 0.005
HR 5467	37.4 ± 0.2	33.4 ± 0.2	0.999 ± 0.008
HR 6348	234.7 ± 0.4	209.2 ± 0.8	1.000 ± 0.004
HR 7018	37.3 ± 0.2	32.8 ± 0.2	1.012 ± 0.007
HD 41371	116.5 ± 0.3	103.7 ± 0.1	1.002 ± 0.003
HD 166780	237.0 ± 0.6	212.1 ± 0.6	0.996 ± 0.004
HD 173511	247.1 ± 0.3	219.0 ± 1.0	1.006 ± 0.004
BD+16 1644	77.4 ± 2.6	71.5 ± 0.4	0.965 ± 0.033

Figure 2 plots the last column of Table 3 as a function of Red PU photometry in the top panel. The line fitted to the data accounts for the uncertainties, and its slope deviates from the horizontal by only 0.3 σ. We can conclude that the responsivity of the Red PU array behaves linearly over the flux range considered.

The bottom panel of Figure 2 tells a different story. Here, the analysis is based on the older S18.7 pipeline output. The S18.7 pipeline version did not provide the new "acqr.fits" files. Instead, it provided "bcd.fits" files, which are not processed as thoroughly.[1] Ludovici et al. (2011) presented a linearity analysis of the Red PU data at the Seattle meeting of the AAS based on the S18.7 data, and they concluded that in fact the data do deviate from a linear response, with fainter targets showing a slightly smaller response than brighter targets.

Our analysis of the S18.7 data reveals a shift of ∼1.0%. The slope deviates from the horizontal at a 3-σ confidence level, which while not definitive does support the earlier conclusion. We conclude that the new "acqr.fits" files released with the S18.18 pipeline show a linear response function, but the "bcd.fits" files available with older pipelines may not be as robust.

[1]Interestingly, no "bcd.fits" files for the PU acquisition data are available in the S18.18 pipeline release.

References

Engelbracht, C. W., et al. 2007, *PASP*, **119**, 994.

Houck, J.R., et al. 2004, *ApJS*, **154**, 18.

Ludovici, D., Sloan, G.C., Barry, D.J., Lebouteiller, V., Bernard-Salas, J., & Spoon, H.W.W. 2011, "Characterization and Calibration of the Infrared Spectrograph on the *Spitzer Space Telescope*," *BAAS*, Abstract 254.22.

Rieke, G. H., et al. 2008, *AJ*, 135, 2245.

Sloan, G.C., & Ludovici, D.A. 2011, "IRS-TR 11001: Temporal Responsivity Variations on the Red Peak-Up Sub-Array."

Werner, M.W., et al. 2004, *ApJS*, **154**, 1.